Power Management for Self-Powered SiC Based AC Smart-Breaker for Nano-grid Applications

Masafumi Otsuka, David K.W. L and Olivier Trescases
University of Toronto
10 King's College Road
Toronto, Canada
Phone: +1 (416) 978-2274
Fax: +1 (416) 971-2325
Email: masafumi.otsuka@utoronto.ca

KEYWORDS

≪SiC≫, ≪Energy system management≫, ≪Smart microgrids≫.

ABSTRACT

This work targets a novel self-powered Smart Circuit Breaker (SCB) for monitoring and controlling power in emerging small-scale AC nano-grids. The SCB concept is intended as a direct replacement of standard(120 Vac, 15 Arms) household circuit breakers, which imposes several challenging constraints. The SCB must therefore generate its own internal supply from the small AC voltage drop across the main switch when the breaker is closed. The SCB is composed of the following key blocks: 1) back-to-back 900 V Silicon Carbide (SiC) MOSFETs as the main power switches, 2) a low-voltage energy harvesting circuit, 3) a high-voltage step-down converter, and 4) low-power digital controller and wireless communication circuits. In order to stabilize the internal supply voltage under a wide range of AC load currents, a novel approach of dynamic on-resistance control is implemented, through adaptive gate-drive and MOSFET segmentation. The fabricated SCB prototype dissipates only 7.4 W for a 13 Arms AC load, corresponding to an efficiency of 99.5%.

I. INTRODUCTION

With an estimated 1.2 billion people living without reliable access to electricity, deploying power-grid infrastructure to rural and remote communities is one of the major challenges of the 21st century [1] [2]. Small-scale AC nano-grids, encompassing an area as small as a single home, can be used to gradually scale up the power generation capacity, as shown in Fig. 1 [3]. There are several key enabling technologies for nano-grids based on renewable energy, including low-cost power electronics hardware such as dc-ac micro-inverters for photovoltaic (PV) and battery modules. At the heart of each nano-grid is an Intelligent Distribution Panel (IDP) [3] that serves to monitor and regulate solar generation, storage, and loads. Within the IDP is an array of Smart Circuit Breakers (SCB), which is the main focus of this paper. The SCB performs current monitoring, protection and load-shedding on each AC load circuit. The nano-grid architecture may be viewed as one form of the so-called Internet of Energy, due to its many similarities with the telecommunications Internet. Such scalable nano-grids can provide rural communities with reliable electrical power with a reduced capital cost.

While the primary objective of nano-grid technology is to address rural electrification, the development of a high-performance SCB will also benefit urban installations connected to the existing grid. In recent years, several companies have begun providing energy management systems to residential and commercial users that can greatly benefit from SCBs [4]. The SCB's ability to shed loads during peak billing periods enhances grid stability and reduces utility costs. The SCBs can be further developed to form resilient power islands during grid failures, which is of particular importance to communities in areas prone to natural disasters.

The paper is organized as follows. Section II outlines the proposed smart breaker concept. Section III describes the key operating modes. Simulation and experimental results for the prototype are reported in Section IV. Finally, conclusions are presented in Section V.

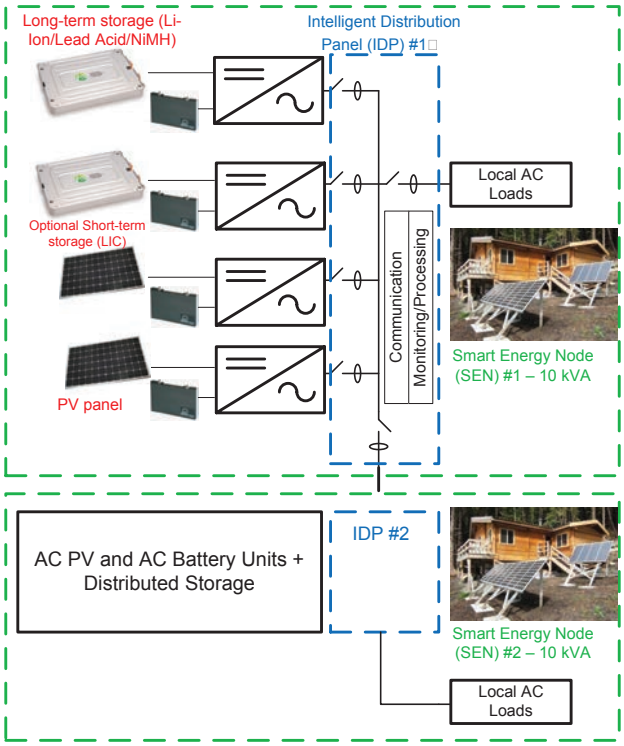

Fig. 1. Nano-grid architecture [3].

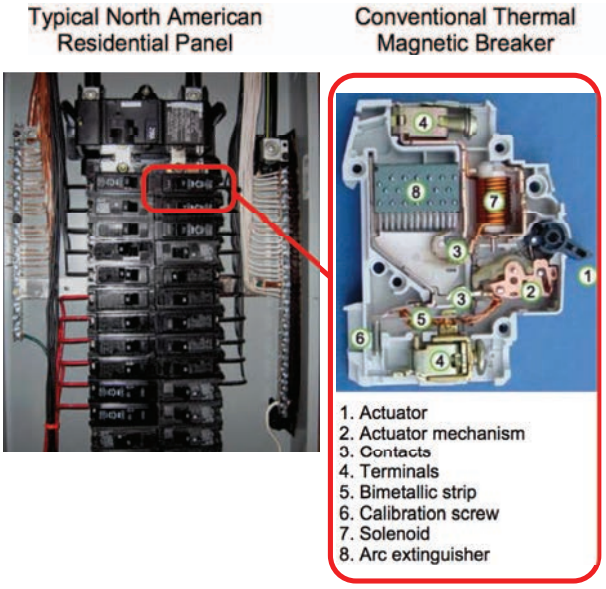

Fig. 2. Residential panel and conventional circuit breaker.

II. Proposed Smart Circuit Breaker Concept

The conventional AC residential circuit breaker and typical distribution panel are shown in Fig. 2. The conventional circuit breaker uses a bimetallic strip as the main switch. The trip-current accuracy and delay are generally far inferior to solid-state solutions. Most importantly, in the context of a nano-grid, the switch is not electronically controllable nor is the current measurement externally available.

The electronic circuit breaker shown in Fig. 3 [3] contains 1) Hall-effect sensors for current measurement, 2) an electro-mechanical relay for load control and 3) all the signal-conditioning and data converters needed for high-precision current sampling and harmonic analysis. While this electronic circuit breaker is reasonably compact and has extremely low conduction loss, there are several critical limitations: the low level of on-chip integration leads to a high mass-production cost, 2) the mechanical relay is slow and suffers from poor lifetime, and most notably 3) external auxiliary power must be supplied to the control circuits, which adds to cost and makes the breaker incompatible as a drop-in replacement in existing residential distribution panels.

The purpose of this project is to address these limitations by developing a novel SCB architecture with the following requirements:

1) High-efficiency (below 10 W conduction loss at 15 Arms) solid-state AC switch with for fast load-shedding and Soft-switching for improved high-reliability.
2) Accurate current sensing.
3) Low-power wireless communication.
4) Compatible with future on-chip integration, with the goal to achieve the same physical footprint as existing AC breakers.
5) Self-powered, with no additional power or communication wires needed compared to existing circuit breakers.

Amongst the aforementioned requirements, points 2 and 3 can be realized using off-the-shelf solutions. For example, in this work, a low R_{on}, Hall Effect integrated current sensor and a 4.5 mW Bluetooth Low Energy transceiver are used to relay the cycle-by-cycle line information back to the Bridge. Solutions to points 1, 4, and 5, however, are not obvious and are the main focus of this paper.

Given the severely constrained physical footprint of existing AC breakers, the first requirement is met by using

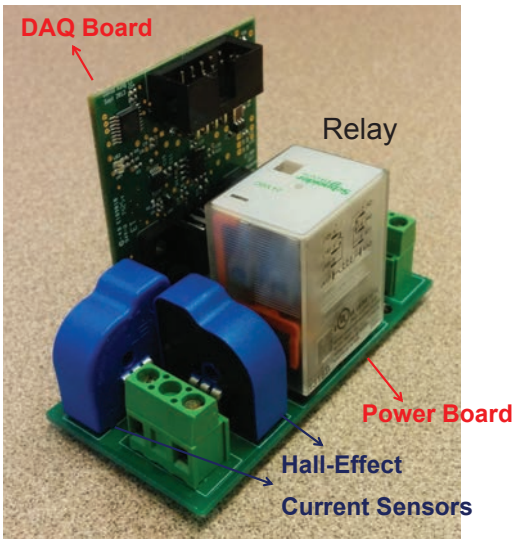

Fig. 3. Relay-based electronic breaker [3].

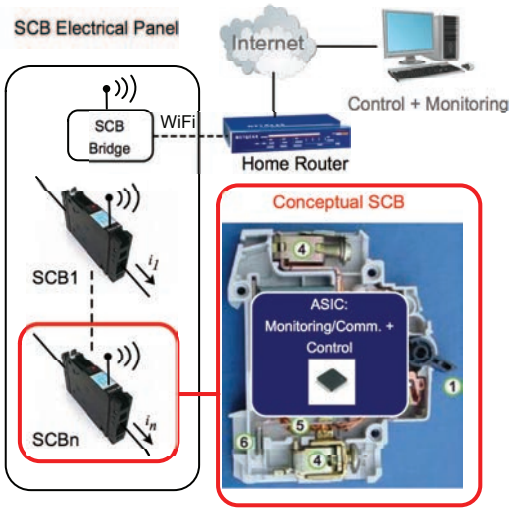

Fig. 4. Proposed smart breaker concept.

new SiC MOSFET technology, as described in Section II-B. The last requirement is particularly challenging and necessitates an innovative power management approach: the SCB must generate its auxiliary power directly from the voltage that appears across the two SCB terminals, without access to the AC neutral connection. The auxiliary power must be tightly regulated both in the breaker closed and open states, as described in Section II-B.

A. Power Switch

The characteristics of several candidate switches for SCBs operating up to 240 Vac are listed in Table I. Since reverse-blocking is needed in the SCB, both MOSFETs and IGBTs must be connected in a back-to-back configuration, which effectively doubles the conduction losses. Due to the vastly superior $R_{on}A$ Figure-of-Merit, SiC MOSFETs [5] can achieve a conduction loss below 7.4 W with 15 Arms in a PCB area below 1400 mm^2, which is 1.8$\times$ lower than the Silicon MOSFET solution. Developing a custom multi-chip SiC module with eight dice would further reduce the area, since the total die area for eight SiC 32.5 $m\Omega$ MOSFETs is only 35 mm^2. There are no existing IGBT or TRIAC based solutions that can meet the 10 W maximum loss requirement. GaN devices could further reduce the area and loss, but their cost is prohibitive in this application.

TABLE I
SCB CANDIDATE SWITCH CHARACTERISTICS

Performance	Si	SiC	IGBT	TRIAC	Units
Part Number	IPW65R080CFD	C3M0065090J	STGWT20H65FB	BTA225B	
Voltage rating	700	900	650	800	V
Voltage Drop at 15 A	0.54	0.49	1.55	1.2	V
Power Loss at 15 Arms	8.1	7.31	23.25	18	w
Total Package Area	2610	1400(35)	251	162	mm^2
Configuration	4 parallel, 2 series	4 parallel, 2 series			

B. SCB Power Management

The proposed high-level SCB concept is shown in Fig. 4, where each SCB monitors and controls one load circuit and communicates wirelessly to a Bridge within the IDP. The Bridge provides a direct link to the Internet for management of the nano-grid via the Cloud.

The simplified SCB architecture, shown in Fig. 5, consists of 1) back-to-back SiC MOSFETs, 2) high-voltage buck converter for regulating the internal supply, V_{aux}, during breakers open state, 3) an ultra low-power boost

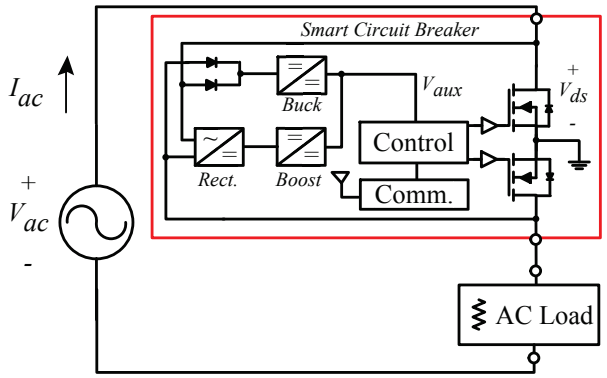

Fig. 5. Proposed high-level SCB concept.

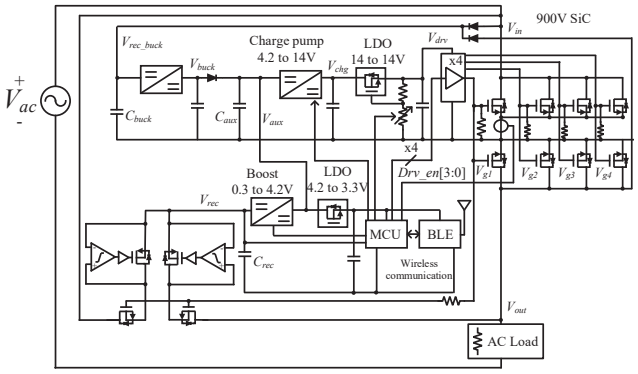

Fig. 6. Detailed architecture of the proposed SCB.

converter fed by an active rectifier for regulating the internal supply during the breakers closed state, 4) sensing, control and communication circuits. A more detailed architecture for the discrete prototype is shown in Fig. 6. Note that most of the functions can be integrated on-chip for future miniaturization, which is beyond the scope of this paper. The internal ground of the SCB is the source node of the power MOSFETs. The two power-management modes are described as follows:

1) Breaker OPEN; Buck Mode: While the breaker is open, the full AC voltage, V_{ac}, appears across V_{in} and V_{out}. The buck converter is fed with the diode-rectified V_{ac} to generate V_{aux}. The buck converter operates in hysteretic voltage mode, with a very large conversion ratio to step the 120 Vrms input down to 4.8 V. The buck converter output supplies the low-voltage control circuits through a 3.3 V linear regulator. A charge pump boost circuit is used to generate a 14 V drive voltage from the buck converter output for the SiC MOSFETs.
2) Breaker CLOSED; Boost Mode: While the breaker is closed, the only voltage available for auxiliary supply generation is the on-state drop across the power MOSFETs, $V_{ds} = I_{ac} \cdot 2R_{on}$, which is designed to be very low to reduce conduction losses. Adding further complexity is the fact that the voltage drop is dependent on the rapidly changing AC load conditions. To address this, an active rectifier, with a similar architecture to wireless power transfer circuits [6], is used to create a low voltage DC output. This low voltage DC then feeds into a high step-up ratio, ultra low-power boost converter [7] to generate V_{aux}.

During the breaker closed state, the MOSFET voltage drop, V_{ds}, is actively controlled to ensure the rectifier output, V_{rect}, is sufficiently high in the presence of the AC load current variations, as shown in Fig. 7. Two variables are used to control the effective R_{on}: 1) the drive voltage, V_{drv}, is controlled via a digital potentiometer on the feedback path of the LDO in Fig. 6, and 2) the effective W/L of the power-stage is controlled by selectively enabling the segmented MOSFETs with $Drv\_en[3:0]$. Using this approach, the effective R_{on} of the SCB can vary across different load conditions, while maintaining constant percentage loss (i.e.: if V_{ds} is approximately independent of load current).

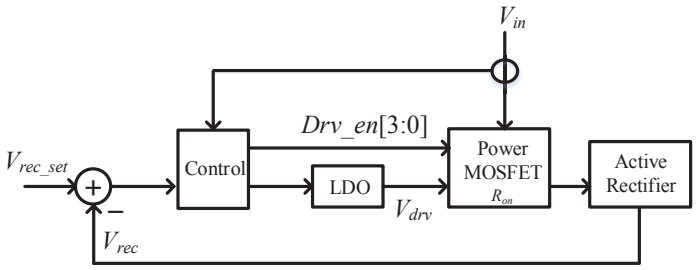

Fig. 7. Gate-drive voltage swing control scheme.

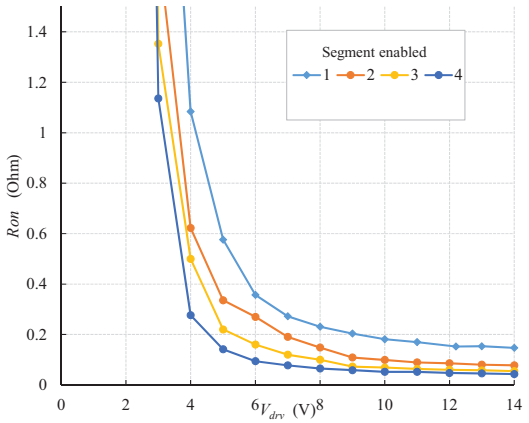

Fig. 8. R_{on} for different number of enabled SiC segments.

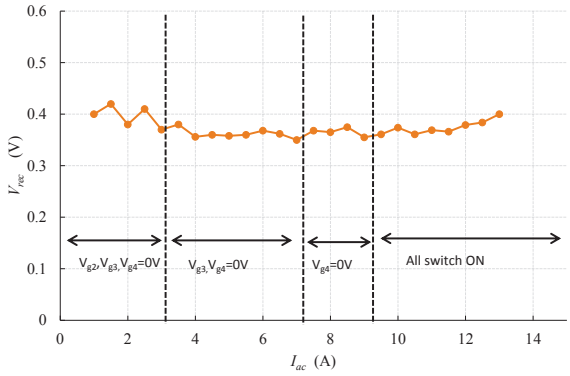

Fig. 9. Measured output of the active rectifier, V_{rec}, for different load currents.

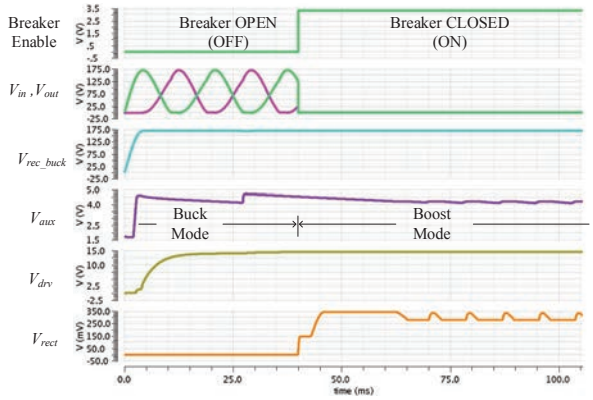

Fig. 10. Simulated cold-start waveform for the SCB.

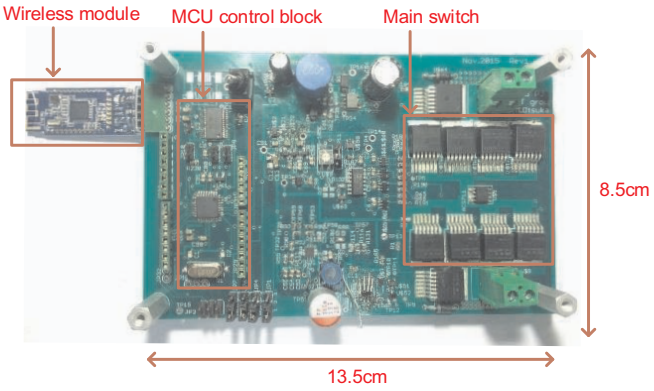

Fig. 11. Experimental SCB prototype rated for 120 Vac, 15 Arms.

When AC line current is periodic, the output of the active rectifier, V_{rec}, is given by

$$V_{rec} = \frac{R_{on} I_{pk}}{K} - R_{rec} I_{boost}, \tag{1}$$

where K is the number of SiC segments enabled, I_{pk} is the peak current of AC load, R_{rec} is the series resistance including active rectifier and clamp MOSFET's on resistance and I_{boost} is the input current of boost circuit. The R_{on} is given by

$$R_{on} = \frac{1}{\beta(V_{drv} - V_{th})}, \tag{2}$$

where V_{th} is the SiC threshold voltage and β is the transistor gain factor. The measured measured R_{on} at each segment enabled condition is shown in Fig. 8. Equations (1) and (2) are the theoretical foundations of this work. In order to avoid the energy harvesting boost converter from collapsing due to low input voltage at V_{rec} [8], the SCB has to maintain sufficient voltage across the AC line as stated in (1). This control mechanism is implemented by controlling R_{on} via V_{drv} and K as stated in (1)-(2). Fig. 9 illustrates the measured V_{rec} at each load condition. The number of enabled segments is chosen based on the load current; all segmented are enabled beyond 9 Arms. All switch turn on more than 9 Arms.

III. Cold-Start Simulation Result

This sections covers the cold-start operation, where a fully discharged SCB is connected to the AC line for the first time following an outage. The simulated cold-start process is illustrated in Fig. 10. When the breaker is open, the diode rectifier passively serves as a startup energy harvester until its rectified output, V_{rec_buck} , reaches 169 V. The second stage buck converter then takes power from V_{rec_buck} to produce V_{aux}, the node that supplies the

main control and gate drive circuits. When V_{aux} comes online, the downstream charge pump regulates V_{chg} to 15 V and the controller proceeds to enable to turn on the SiC MOSFETs. It can be seen in Fig. 10 that, as the breaker is closed,the terminal voltage of the SCB, V_{in}, decreases to 340 mVac with a 15 Arms load. Simultaneously, the diode rectifier automatically turns off and the on-board controller begins to actively rectify the 340 mVac input to bring up V_{rec}. At this point, the boost circuit regulates V_{aux} in lieu of the buck converter.

IV. Experimental Results

An experimental SCB prototype was built to demonstrate the power power management scheme of Fig. 6. The main AC line switch is composed of eight SiC devices, as shown in Fig. 11. These devices, along with the electrolytic capacitors C_{buck} and C_{rec}, dominate the PCB volume; however the volume of these components is expected to decrease in an integrated SCB solution. The capacitance C_{buck}, in particular, can be reduced if the buck converter is implemented with a more sophisticated current-mode control, instead of the basic hysteretic voltage mode control used in this prototype. The measured cold-start process discussed in Section III is shown in Fig. 12. When the SCB is connected to the AC grid in the open state, the buck converter starts running to generate 4.8 V. Following the MCU startup, the charge-pump operates to generate V_{drv}. When the breaker is closed, the rectifier feeds V_{rec}, as shown in Fig. 13. Due to the current limit of the AC power supply, all measurements were performed up to 13 Arms.

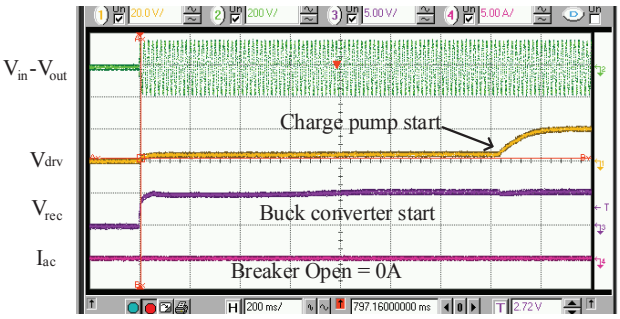

Fig. 12. Measured SCB startup waveforms for an AC input 120 Vac in the open state.

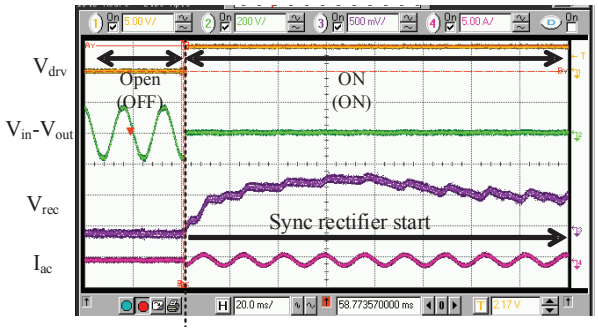

Fig. 13. Measured SCB waveforms for an AC input 120 Vac when breaker is closed .

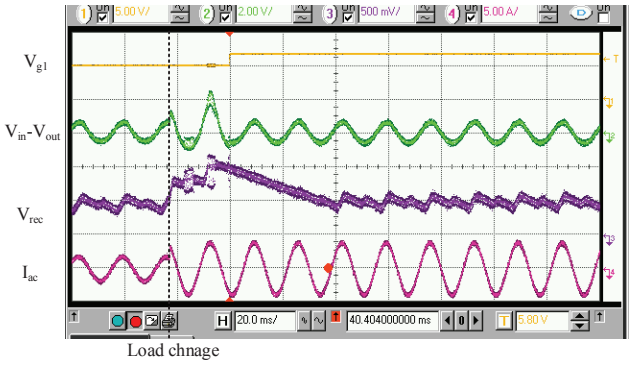

Fig. 14. Load transient (1 Arms to 2.5 Arms) when the breaker is closed with 1 segment enabled.

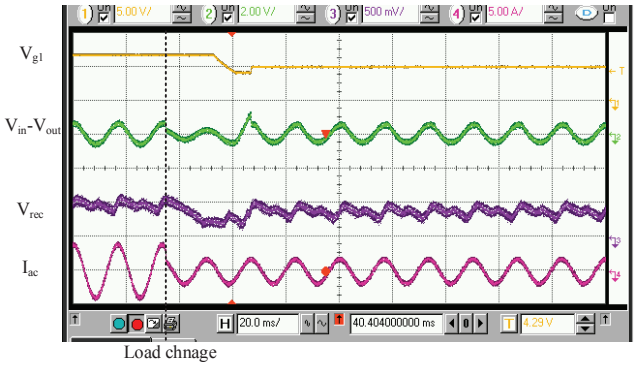

Fig. 15. Load transient (2.5 Arms to 1 Arms) when the breaker is closed with 1 segment enabled.

The on-state voltage drop management scheme proposed in Section II-B is demonstrated in Fig. 14. When a low-power load is connected (1 Arms in this case), the controller lowers the gate-drive voltage, V_{drv} to 5 V and uses one segment. When load is changed to 2.5 Arms, the controller increase the gate-drive voltage, V_{drv} to 7.1 V and also uses just a single segment in this case. When load is further reduced, V_{drv} returns to previous voltage, as shown in Fig. 15. For larger loadpstep of 13 Arms, the controller adjusts the number of segment enabled SiC devices as well as the gate-voltage, as shown in Fig. 16. V_{g2}, V_{g3} and V_{g4} decrease for a load-step of 13 to 1 Arms

in Fig. 17. When the load increases, the gate drive voltage increases and SiC switches are re-enabled accordingly to optimize the conduction losses while maintaining the energy harvesting operation. The measured infrared thermal profile is shown in Fig. 18. The maximum temperature is 77 °C and with a loss of 7.4 W, which is below the target 10 W. The measured efficiency of the SCB is shown in Fig. 19. The efficiency is over 99%.

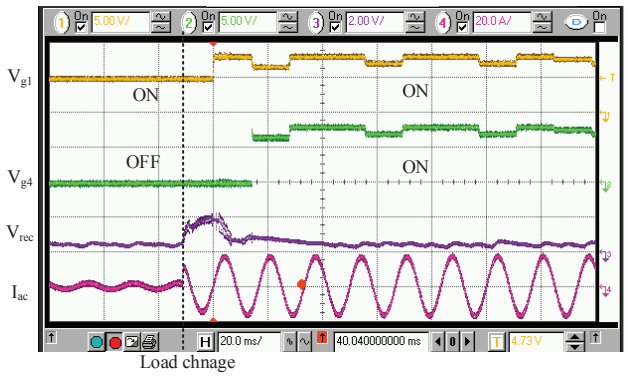

Fig. 16. Load transient (1 Arms to 13 Arms) when the breaker is closed with 4 segments enabled.

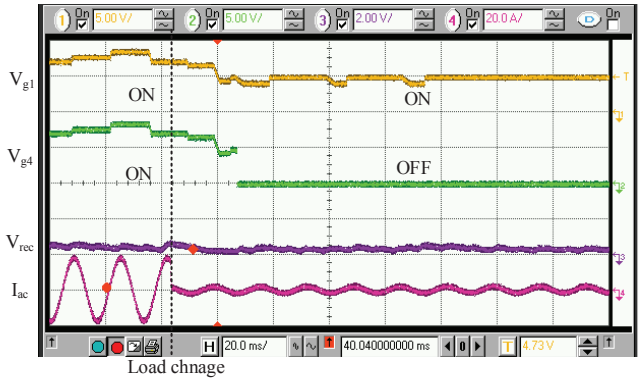

Fig. 17. Load transient (13 Arms to 1 Arms)when the breaker is closed with 4 segments enabled.

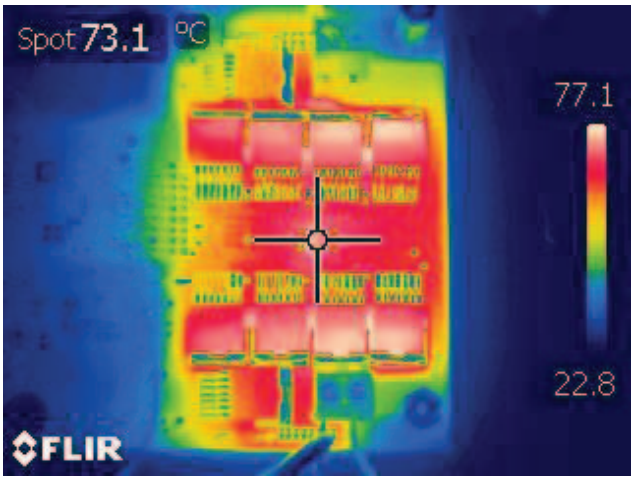

Fig. 18. Measured infrared thermal profile of the SCB for a load current of 13 Arms.

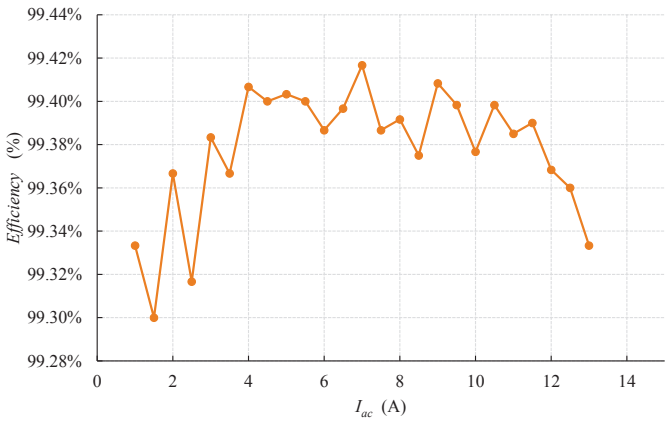

Fig. 19. Measured SCB efficiency.

V. Conclusions

The SiC based SCB prototype meets the sub 10 W power specification and successfully generates the internal supply voltage under a variety of load conditions, in both the breaker closed and open states. The main contribution of this work is the on-state voltage drop management through adaptive drive voltage and MOSFET segmentation. Further on-chip integration of the power management and control circuits is needed to achieve the vision of a drop-in replacement for existing passive circuit breakers.

References

[1] S. Rolland and G. Glania, "Hybrid mini-grids for rural electrification: Lessons learneds," *Alliance for Rural Electrification*, 2011.

[2] "What we do: Achieving universal energy access," United Nations Foundation, available http://www.unfoundation.org/what-we-do/issues/energy-and-climate/clean-energy-development.html.

[3] D. Li, S. Poshtkouhi, O. Trescases, R. Orr, and B. Bacque, "Intelligent ac distribution panel for real-time load analysis and control in small-scale power grids with distributed generation," in *Humanitarian Technology Conference (IHTC2015), 2015 IEEE Canada International*, May 2015, pp. 1–4.

[4] "Eaton energy mnagement system upgrad kit." IXYS Datasheet, available at http://www.eatonguard.com/datasheets/EMS-UpgradeKit.pdf.

[5] S. Safari, A. Castellazzi, and P. Wheeler, "Performance evaluation of bidirectional sic switch devices within matrix converter," in *Power Electronics and Applications (EPE), 2013 15th European Conference on*, Sept 2013, pp. 1–9.

[6] Y. Sun, C.-J. Jeong, S.-K. Han, and S.-G. Lee, "A high speed comparator based active rectifier for wireless power transfer systems," in *Intelligent Radio for Future Personal Terminals (IMWS-IRFPT), 2011 IEEE MTT-S International Microwave Workshop Series on*, Aug 2011, pp. 1–2.

[7] "Ultra low-power boost converter with battery management for energy harvester applications," TI datasheet, available http://www.ti.com/lit/ds/symlink/bq25504.pdf.

[8] J. Kimball, T. Flowers, and P. Chapman, "Low-input-voltage, low-power boost converter design issues," *Power Electronics Letters, IEEE*, vol. 2, no. 3, pp. 96–99, Sept 2004.